Fig. 4. Depletion of HeLa S10 by pre-immune IgG and affinity purified anti-PTB IgG. They were reacted with anti-PTB antibody by WB. Asterisk indicates the position of PTB proteins. Anti-PTB IgG deplete 94.5% of PTB (lane PTB) and pre-immune IgG deplete 26.3% of PTB (lane pre).

shown). This might indicate the existence of several translation factors other than PTB, which were lost during the treatment of IgG.

Taken together, results of this study strongly indicate that significance of PTB was highest in PV-IRES and was lowest implication in HCV-IRES.

4. Discussion

In present study, the significance of PTB in HCV, EMCV and PV IRESs has been compared. From the immuno-depletion experiment (Table 1), PTB-Ig depleted S10 (4.0 μl) contained 0.009 molecule of PTB per 1 molecule of RNA, in which PV IRES activity is 0.9%. This may indicate that almost one PTB molecule should be required

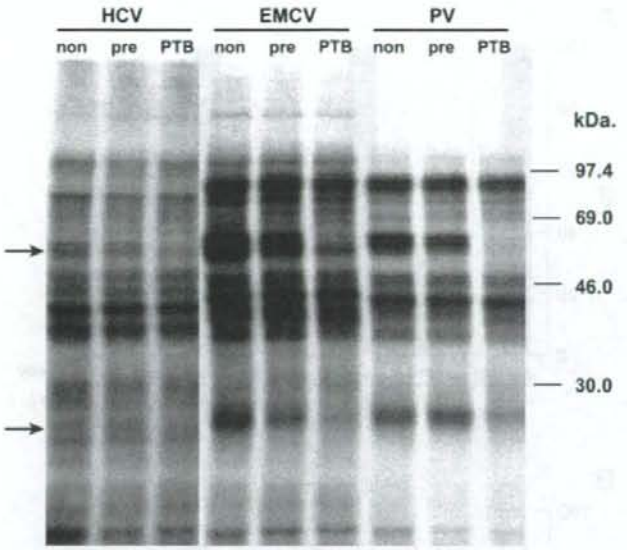

Fig. 5. UV-cross-linking analysis of HCV, EMCV and PV RNA with non-treated, pre-immune IgG-treated, and anti-PTB IgG-treated HeLa S10 lysate (lane non, pre, PTB). Upper arrow indicates the binding of PTB. Doublet protein (57 and 60 kDa) was decreased, especially in PV-RNA. Lower arrow indicates 28 kDa protein.

for 100% activity of PV IRES-RNA. In the case of EMCV IRES-RNA, 0.002 molecule of PTB per RNA gave 11% of EMCV IRES activity, and that of HCV IRES, 0.0025 molecule of PTB gave 31% of HCV IRES activity. Therefore, requirement of PTB for IRES activity was highest in PV, and less in EMCV and HCV IRES-RNA.

From the results in this study, we can compare the requirement amount of PTB in IRES activity with those of canonical eIFs. The most limiting initiation factor in cells is eIF4E, with estimates in rabbit reticulocyte lysates ranging from 0.02 copies [23] to 1 copy [24] per ribosome. The concentration of ribosomes has been estimated to be approximately 2 μM [25]. From the results of *in vitro* translation experiment, PTB should work at 0.1–0.15 M in each IRESs at maximum activity (Table 1). Therefore, working concentration of PTB for IRES activity should show almost similar to those of eIFs.

During the immuno-depletion experiment, treatment of normal IgG conjugated beads decreased the IRESs activity; 89 (6.5 μl) or 33 (3.5 μl)% in HCV IRES, 53 or 28% in EMCV IRES, and 22% or 15% in PV-IRES (Table 1). This may suggest the existence of unknown factors, which could be inactivated during the process of immuno-depletion experiment, and these effects in PV-IRES were highest among the IRESs. PV-IRES is classified into the type I [26], and the canonical eIFs with the exception of cap-binding protein eIF4E [27] and PTB [26], La [26] and 39 kDa poly(rC)-binding protein [26] are working. In EMCV IRES (type II), eIF4G was

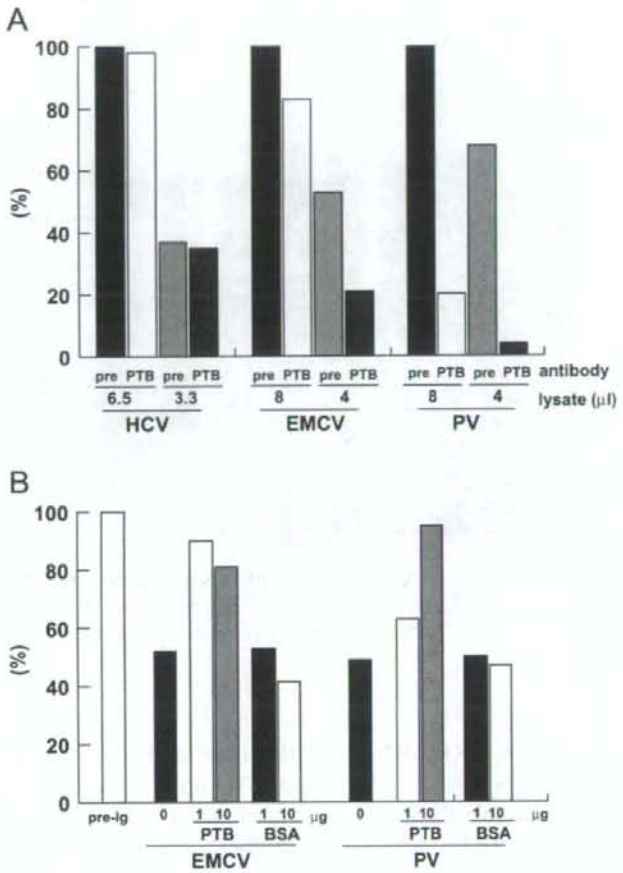

Fig. 6. (A) Effect of PTB depletion in HCV, EMCV and PV IRES. IRESs were translated in pre-immune IgG-depleted and anti-PTB IgG depleted S10 lysates (3.3, 6.5 μl in HCV-IRES, 4.0, 8.0 μl in EMCV- and PV-IRES. Translated products in SDS-PAGE were measured by image analyzer, and the quantity (PSL) of pre-immune IgG-treated S10 lysate was calculated as 100%. (B) Recovery of translation in PTB depleted S10 lysate by addition of recombinant PTB protein (1 and 10 μg. Translated products in SDS-PAGE were measured by image analyzer, and the quantity (PSL) of pre-immune IgG-treated S10 lysate was calculated as 100%.

directly bound and eIF4A and eIF4B can recruit 43S preinitiation complex which is composed of 40S ribosomal subunit and eIF3, eIF2, GTP and initiator tRNA[13]. Recent findings indicated the dependence of EMCV IRES on PTB for activity [28]. The HCV IRES possesses striking difference from type I and II IRESs, it recruits 43S preinitiation complex to initiation codon to form a 48S complex without involvement of eIF4A, 4B or 4F [29]. Thus, HCV IRES is simple and does not require most of eIFs, and might not be influenced by the depletion experiment using normal IgGs.

Table 1
Effect of PTB depletion in HCV, EMCV and PV IRES

RNA	RNA quantity (pmol)	S10 (μl)	PTB (ng)	Molar ratio of PTB to RNA	Ratio of translation (%)[a]
HCV	1.0	*Untreated*			
		6.5	7.2	0.12	100
		3.5	3.6	0.06	63
		Pre-im.-IgG			
		6.5	5.2	0.085	89
		3.5	2.6	0.045	33
		αPTB-IgG			
		6.5	0.4	0.005	87
		3.5	0.2	0.0025	31
EMCV	1.8	*Untreated*			
		8.0	8.8	0.08	100
		4.0	4.4	0.04	57
		Pre-im.-IgG			
		8.0	6.4	0.06	53
		4.0	3.2	0.03	28
		αPTB-IgG			
		8.0	0.5	0.005	44
		4.0	0.2	0.002	11
PV	0.36	*Untreated*			
		8.0	8.8	0.4	100
		4.0	4.4	0.2	65
		Pre-im.-IgG			
		8.0	6.4	0.3	22
		4.0	3.2	0.15	15
		αPTB-IgG			
		8.0	0.5	0.02	4.5
		4.0	0.2	0.009	0.9

[a]Ratio of translation products was quantitated by image analyzer.

Recent riboproteomic approach revealed the novel interacting proteins to IRESs [30], other than PTB, such as actin, forming homolog overexpressed in spleen, and microtuble interacting protein that associates with TRAF3. These factors should be characterized as novel ITAFs and comparative aspects in different IRESs should be addressed in the future work to clarify the character of each IRESs.

Acknowledgments

This work was supported by the grants from the Ministry of Health and Welfare, or Education, Culture, Sports, Science and Technology of Japan, the program for

promotion of fundamental studies in health sciences of the National Institute of Biomedical Innovation, and the Cooperative Research Project on Clinical and Epidemiological Studies of Emerging and Re-emerging Infectious Diseases.

References

[1] Choo QL, Kuo G, Weiner AJ, Overby LR, Bradley DW, Houghton M. Isolation of a cDNA clone derived from a blood-borne non-A, non-B viral hepatitis genome. Science 1989;244:359–62.
[2] Takamizawa A, Mori C, Fuke I, Manabe S, Murakami S, Fujita J, et al. Structure and organization of the hepatitis C virus genome isolated from human carriers. J Virol 1991;65:1105–13.
[3] Kato N, Hijikata M, Ootsuyama Y, Nakagawa M, Ohkoshi S, Sugimura T, et al. Molecular cloning of the human hepatitis C virus genome from Japanese patients with non-A, non-B hepatitis. Proc Natl Acad Sci USA 1990;87:9524–8.
[4] Kaito M, Watanabe S, Tsukiyama-Kohara K, Yamaguchi K, Kobayashi Y, Konishi M, et al. Hepatitis C virus particle detected by immunoelectron microscopic study. J Gen Virol 1994;75(Part 7):1755–60.
[5] Tsukiyama-Kohara K, Iizuka N, Kohara M, Nomota A. Internal ribosome entry site within hepatitis C virus RNA. J Virol 1992;66:1476–83.
[6] Kamoshita N, Tsukiyama-Kohara K, Kohara M, Nomoto A. Genetic analysis of internal ribosomal entry site on hepatitis C virus RNA: implication for involvement of the highly ordered structure and cell type-specific transacting factors. Virology 1997;233:9–18.
[7] Nomoto A, Tsukiyama-Kohara K, Kohara M. Mechanism of translation initiation on hepatitis C virus RNA. Princess Takamatsu Symp 1995;25:111–9.
[8] Pelletier J, Sonenberg N. Internal initiation of translation of eukaryotic mRNA directed by a sequence derived from poliovirus RNA. Nature 1988;334:320–5.
[9] Kieft JS, Zhou K, Jubin R, Doudna JA. Mechanism of ribosome recruitment by hepatitis C IRES RNA. RNA 2001;7:194–206.
[10] Yu Y, Ji H, Doudna JA, Leary JA. Mass spectrometric analysis of the human 40S ribosomal subunit: native and HCV IRES-bound complexes. Protein Sci 2005;14:1438–46.
[11] Hellen CU, Pestova TV, Litterst M, Wimmer E. The cellular polypeptide p57 (pyrimidine tract-binding protein) binds to multiple sites in the poliovirus 5′ nontranslated region. J Virol 1994;68:941–50.
[12] Hunt SL, Jackson RJ. Polypyrimidine-tract binding protein (PTB) is necessary, but not sufficient, for efficient internal initiation of translation of human rhinovirus-2 RNA. RNA 1999;5:344–59.
[13] Kolupaeva VG, Pestova TV, Hellen CU, Shatsky IN. Translation eukaryotic initiation factor 4G recognizes a specific structural element within the internal ribosome entry site of encephalomyocarditis virus RNA. J Biol Chem 1998;273:18599–604.
[14] Kolupaeva VG, Hellen CU, Shatsky IN. Structural analysis of the interaction of the pyrimidine tract-binding protein with the internal ribosomal entry site of encephalomyocarditis virus and foot-and-mouth disease virus RNAs. RNA 1996;2:1199–212.
[15] Sizova DV, Kolupaeva VG, Pestova TV, Shatsky IN, Hellen CU. Specific interaction of eukaryotic translation initiation factor 3 with the 5′ nontranslated regions of hepatitis C virus and classical swine fever virus RNAs. J Virol 1998;72:4775–82.
[16] Witherell GW, Wimmer E. Encephalomyocarditis virus internal ribosomal entry site RNA–protein interactions. J Virol 1994;68:3183–92.
[17] Scheper GC, Voorma HO, Thomas AA. Binding of eukaryotic initiation factor-2 and trans-acting factors to the 5′ untranslated region of encephalomyocarditis virus RNA. Biochimie 1994;76:801–9.
[18] Ali N, Siddiqui A. Interaction of polypyrimidine tract-binding protein with the 5′ noncoding region of the hepatitis C virus RNA genome and its functional requirement in internal initiation of translation. J Virol 1995;69:6367–75.
[19] Jang SK, Wimmer E. Cap-independent translation of encephalomyocarditis virus RNA: structural elements of the internal ribosomal entry site and involvement of a cellular 57-kDa RNA-binding protein. Genes Dev 1990;4:1560–72.

[20] Luz N, Beck E. Interaction of a cellular 57-kDa protein with the internal translation initiation site of foot-and-mouth disease virus. J Virol 1991;65:6486–94.
[21] Jang SK, Pestova TV, Hellen CU, Witherell GW, Wimmer E. Cap-independent translation of picornavirus RNAs: structure and function of the internal ribosomal entry site. Enzyme 1990;44:292–309.
[22] Garcia-Blanco MA, Jamison SF, Sharp PA. Identification and purification of a 62,000-Da protein that binds specifically to the polypyrimidine tract of introns. Genes Dev 1989;3:1874–86.
[23] Hiremath LS, Webb NR, Rhoads RE. Immunological detection of the messenger RNA cap-binding protein. J Biol Chem 1985;260:7843–9.
[24] Rau M, Ohlmann T, Morley SJ, Pain VM. A reevaluation of the cap-binding protein, eIF4E, as a rate-limiting factor for initiation of translation in reticulocyte lysate. J Biol Chem 1996;271:8983–90.
[25] Duncan R, Hershey JW. Identification and quantitation of levels of protein synthesis initiation factors in crude HeLa cell lysates by two-dimensional polyacrylamide gel electrophoresis. J Biol Chem 1983;258:7228–35.
[26] Flint SJ, Enquist LW, Krug RM, Racaniello VR, Skalka AM, editors. Virology. Washington, DC: ASM Press; 2000.
[27] Gingras AC, Svitkin Y, Belsham GJ, Pause A, Sonenberg N. Activation of the translational suppressor 4E-BP1 following infection with encephalomyocarditis virus and poliovirus. Proc Natl Acad Sci USA 1996;93:5578–83.
[28] Kaminski A, Jackson RJ. The polypyrimidine tract binding protein (PTB) requirement for internal initiation of translation of cardiovirus RNAs is conditional rather than absolute. RNA 1998;4:626–38.
[29] Hellen CU, Pestova TV. Translation of hepatitis C virus RNA. J Viral Hepat 1999;6:79–87.
[30] Lu H, Li W, Noble WS, Payan D, Anderson DC. Riboproteomics of the hepatitis C virus internal ribosomal entry site. J Proteome Res 2004;3:949–57.

Available online at www.sciencedirect.com

ScienceDirect

Virology 375 (2008) 321–330

VIROLOGY

www.elsevier.com/locate/yviro

Measles virus induces cell-type specific changes in gene expression

Hiroki Sato [a], Reiko Honma [b], Misako Yoneda [a], Ryuichi Miura [a], Kyoko Tsukiyama-Kohara [c], Fusako Ikeda [a], Takahiro Seki [a], Shinya Watanabe [b], Chieko Kai [a,*]

[a] *Laboratory Animal Research Center, The Institute of Medical Science, The University of Tokyo, 4-6-1 Shirokanedai, Minato-ku, Tokyo 108-8639, Japan*
[b] *Clinical Informatics, Tokyo Medical and Dental University, 1-5-45 Yushima, Bunkyo-ku, Tokyo, Japan*
[c] *Faculty of Medical and Pharmaceutical Sciences, Kumamoto University, 1-1-1 Honjo, Kumamoto City, Kumamoto, Japan*

Received 16 May 2007; returned to author for revision 13 June 2007; accepted 8 February 2008
Available online 28 March 2008

Abstract

Measles virus (MV) causes various responses including the induction of immune responses, transient immunosuppression and establishment of long-lasting immunity. To obtain a comprehensive view of the effects of MV infection on target cells, DNA microarray analyses of two different cell-types were performed. An epithelial (293SLAM; a 293 cell line stably expressing SLAM) and lymphoid (COBL-a) cell line were inoculated with purified wild-type MV. Microarray analyses revealed significant differences in the regulation of cellular gene expression between these two different cells. In 293SLAM cells, upregulation of genes involved in the antiviral response was rapidly induced; in the later stages of infection, this was followed by regulation of many genes across a broad range of functional categories. On the other hand, in COBL-a cells, only a limited set of gene expression profiles was modulated after MV infection. Since it was reported that V protein of MV inhibited the IFN signaling pathway, we performed a microarray analysis using V knockout MV to evaluate V protein's effect on cellular gene expression. The V knockout MV displayed a similar profile to that of parental MV. In particular, in COBL-a cells infected with the virus, no alteration of cellular gene expression, including IFN signaling, was observed. Furthermore, IFN signaling analyzed *in vitro* was completely suppressed by MV infection in the COBL-a cells. These results reveal that MV induces different cellular responses in a cell-type specific manner. Microarray analyses will provide us useful information about potential mechanisms of MV pathogenesis.

Keywords: Measles virus; Microarray; V protein; IFN signaling; Lymphoid cells; Epithelial cells

Introduction

During measles virus (MV) infection, the virus first enters the host via the respiratory route and replicates in tracheal and bronchial epithelial cells. The virus then enters and replicates in local lymphatic tissues and spreads through the blood to infect a variety of organs. After a latent period lasting between 10 and 14 days, patients develop symptoms, such as fever, coryza, coughing, and conjunctivitis, followed by the appearance of a characteristic rash. Immune responses have been noted to occur at almost the same time the rash fades. Recovery is accompanied by life-long immunity to reinfection. Immunosuppression, including marked lymphopenia, coincides with the appearance of immune activation and lasts for several weeks after apparent recovery (Griffin, 2001). The various pathogenic forms of measles and the different immune responses are a result of the interaction between the host and the virus. There are many *in vitro* studies on the mechanisms that trigger these reactions in MV-infected cells. For example, MV infection induces innate immune and antiviral proteins, including interferon (IFN) production in MV-infected epithelial, endothelial, and glial cells (Dhib-Jalbut and Cowan, 1993; Helin et al., 2001; Noe et al., 1999; Schneider-Schaulies et al., 1993; Vidalain et al., 2002; Yokota et al., 2004). On the other hand, some reports have demonstrated contrary results suggesting that MV does not induce the production of IFN in peripheral blood mononuclear cells (PBMC) (Naniche et al., 2000). Furthermore, recent reports have indicated that a non-structural accessory protein, the V protein, encoded within the phosphoprotein (P) gene, possesses

* Corresponding author. Fax: +81 3 5449 5379.
E-mail address: ckai@ims.u-tokyo.ac.jp (C. Kai).

0042-6822/$ - see front matter © 2008 Elsevier Inc. All rights reserved.
doi:10.1016/j.virol.2008.02.015

IFN-antagonist activity (Ohno et al., 2004; Palosaari et al., 2003; Takeuchi et al., 2003; Yokota et al., 2003). However, there are discrepancies between the various studies and the full picture remains unclear.

High-density DNA microarrays can provide a powerful approach to the profiling of the simultaneous expression of thousands of genes. Previously, Bolt et al. performed DNA microarray analysis with a limited number of human genes, approximately 3000 genes, to monitor any change in the host transcriptional profile of human PBMCs after infection with MV, and found only a few genes to be upregulated by MV infection (Bolt et al., 2002). To obtain a more comprehensive view of the overall effects of MV infection in target cells, we performed DNA microarray analysis containing more than 22,000 human genes of two different cell-types. Experiments were designed to assess gene expression patterns in human epithelial and lymphoid cells, which are the cell-types that are targeted during the pathogenesis of primary MV infection. A significant difference between these cells was observed. More recently, Zilliox et al. reported a microarray analysis of MV-infected dendritic cells and identified numerous genes that were regulated by MV (622 upregulated and 931 downregulated genes) (Zilliox et al., 2006). The profile of altered gene expression in dendritic cells was similar to that in epithelial cells in our results. Interestingly, cell-type specific modulation of the IFN signaling pathway was identified in the present study. In addition, to evaluate the effect of V protein on the modulation of host gene expression, we generated V knockout MV by employing a reverse genetics system and performed microarray analysis. The present study provides an additional comprehensive view of MV effects on different cells.

Results

Preparation of cells and virus

Experiments were designed to assess patterns of gene expression in human epithelial and lymphoid cells, which are the cell-types that are targeted during the pathogenesis of primary MV infection. First, we established a human epithelial cell line that was sensitive to wild-type MV infection. We took 293 human embryonic kidney epithelial-like cells and transfected them with the signaling lymphocytic activation molecule (SLAM) gene, a receptor for wild-type MV (Tatsuo et al., 2001). The cells were highly susceptible to MV infection and showed a large syncytium post infection (data not shown). These cells were designated 293SLAM cells. To compare transcriptional response between different cell-types after MV infection, we used a novel established human lymphoid cell line, COBL-a, which was established from a cultured umbilical cord blood cell colony (Kobune et al., 2007). COBL-a cells are a T cell lineage cell line expressing CD4 (helper-T), CD38 (immature T), CD46, and CD150 (SLAM). Cells are highly sensitive to MV infection and cause CPE post infection. In addition, a wild-type MV isolated from a blood specimen using the COBL-a cells maintained pathogenicity specific for typical acute measles against cynomolgus monkeys. The COBL-a cells are therefore ideal for virus propagation and subsequent microarray assays.

We used the HL strain (Kobune et al., 1996) as a wild-type MV. MV-HL was isolated from blood leukocytes of a patient with typical measles and induced the typical clinical signs of measles, including rashes, Koplik's spots, and transient marked leukopenia in cynomolgus and squirrel monkeys. Thus, MV-HL is considered to possess the pathogenicity of acute measles. The HL strain grew well, both in COBL-a cells and 293SLAM cells, reaching a similar maximum titer in both cells (Fig. 1). Since MV-HL is propagated on B95a cells, a marmoset B-cell line transformed with Epstein–Barr virus (EBV) (Kobune et al., 1990), it was passaged twice in 293SLAM cells that were insensitive to EBV to eliminate EBV in the MV stock solution. The obtained virus solution was inoculated onto COBL-a cells and, after 3 days, no EBV contamination was confirmed by RT-PCR using EBV specific primer pairs (Teng et al., 1996) (data not shown). To obtain the necessary quantity of MV, it was propagated largely in COBL-a cells and was then purified by ultracentrifugation.

Overview of expression microarray analysis

COBL-a cells and 293SLAM cells were inoculated with purified MV at a multiplicity of infection (MOI) of 2 to ensure that every cell was in contact with infectious viral particles. Mock and infected cells were harvested at 6, 12, and 24 h post infection and isolated poly(A+) RNAs were labeled with Cyanine 3-dUTP or Cyanine 5-dUTP. The labeled samples were hybridized on microarrays representing 22,272 human genes. Hybridization signals were processed into expression ratios as log 2 values (designated mean log ratios; see Materials and methods). The genes with mean log ratios over 1 or under −1 in at least one sample were extracted, and cluster analysis was carried out. Data from all the arrays used in this paper are available at DDBJ via CIBEX (http://www.cibex.nig.ac.jp/cibex/HTML/index.html) under accession number CBX32. Interestingly, significant differences in the regulation of cellular gene expression were observed between 293SLAM and COBL-a cells (Fig. 2). The number of genes that were up- and downregulated with a mean log ratio over 1 or under −1 in individual samples is shown in Fig. 2B. In 293SLAM cells,

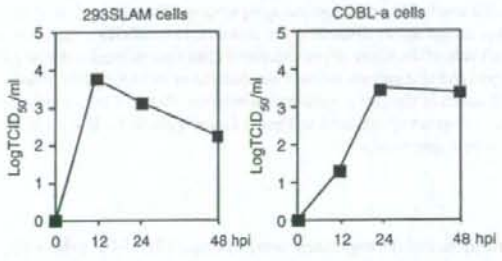

Fig. 1. Comparison of the replication of MV-HL in 293SLAM and COBL-a cells. After infection at an MOI of 0.001, the viral titer was determined by $TCID_{50}$ at the indicated time points. The average of two independent measurements is shown.

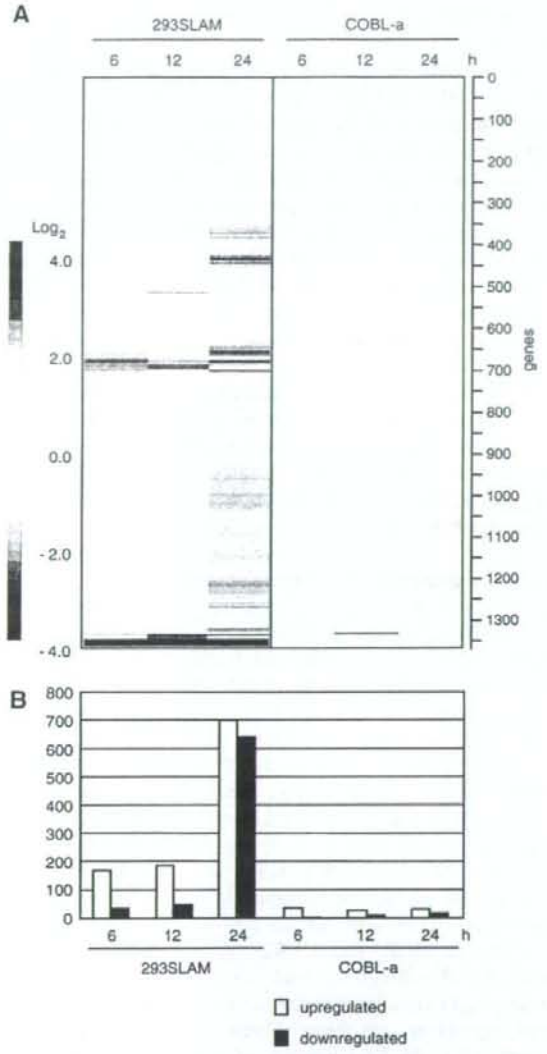

Fig. 2. Gene expression profiles of 293SLAM cells and COBL-a cells inoculated with MV-HL. (A) Genes exhibiting the mean log ratio in all 6 samples were extracted (19,415 genes). These genes were further extracted with |mean log ratio| ≥ 1, and the resulting 1,368 genes were assembled in the order obtained from the results of hierarchical clustering analysis. The y-axis of the dendrogram depicts Euclid square distance as the dissimilarity coefficient. The color bar on the left side of the figure shows expression ratio against mock-infected RNA in $\log_2$; red and blue indicate increase and decrease of mean log ratios, respectively. (B) Kinetics of changes in total gene expression after MV infection. Individual values for genes upregulated and genes downregulated by MV infection were represented graphically.

marked cellular responses were induced by MV infection, and the number of regulated genes increased over time. On the other hand, COBL-a cells showed little alteration in gene expression despite similar viral replication rates as those observed in 293SLAM cells.

Effects of MV on gene expression in 293SLAM cells

In 293SLAM cells, a series of cellular genes was found to be upregulated and downregulated by virus infection. Among genes that were altered early (6 h post infection), the most apparent characteristic was the upregulation of a series of genes that are related to innate immune and antiviral responses. This result clearly showed typical early events after virus infection, such as activation of IRF-3 and NF-kB, which result in the induction of type I IFN. Furthermore, a series of IFN signal transductions was subsequently observed. In particular, the three principal families of IFN-inducible genes (RNA-activated protein kinase [PKR], the 2′5′-oligoadenylate synthetases [OAS], and the Mx proteins) were markedly induced. In addition, activation of a broad range of functional responses that are involved in the host antiviral response, including many IFN-stimulated genes (ISG), inflammatory cytokines, and immune pathways, was demonstrated. These results show that MV infection and replication trigger a rapid and strong innate antiviral response in 293SLAM cells. The number of upregulated genes was slightly increased 12 h post infection (Fig. 2B).

At 24 h post infection, the number of upregulated genes increased significantly; 701 upregulated genes were identified. To facilitate the analysis of our data, we grouped the regulated genes according to biological functions (Table 1). Upregulation

Table 1
Classes of genes upregulated at 24 h post MV infection in 293SLAM cells

Functional classification	Number
Antivirus	60
Metabolism	31
Transcription factor, transcription regulation	30
Zinc finger protein	24
Protein kinases and phosphatases	21
Channels and transporters	18
Nucleus and nuclear matrix	16
Histocompatibility and cell surface markers	15
Oncogenesis	13
Cytoskeleton and cell structure, motor protein	13
Protein degradation	9
Apoptosis, antiapoptosis	9
Cellular development and differentiation, physiology	8
Growth factor	8
RNA processing and binding modification	8
Cell adhesion and intercellular junction, extracellular matrix	7
Cell cycle related	7
Stress response/cell defense	6
Receptor and receptor-associated	6
tRNA	6
DNA modification and replication	5
Vesicular protein trafficking and fusion, vesicular formation	5
Immunity	4
Intracellular transporter	4
Signaling	3
Hormone related	3
Homeostasis	3
Protein modification	1
Translation	1
Unknown function	49
Hypothetical protein	308
Total	701

Table 2
Classes of genes downregulated at 24 h post MV infection in 293SLAM cells

Functional class	Number
Metabolism	108
Protein degradation	35
Cytoskeleton and cell structure, motor protein	27
Ribosomal proteins	26
Protein modification	21
Cellular development and differentiation, physiology	20
Cell adhesion and intercellular junction, extracellular matrix	19
Nucleus and nuclear matrix	19
Transcription factor, transcription regulation	16
Receptor and receptor-associated	14
Protein kinases and phosphatases	11
Channels and transporters	11
Signaling	11
Stress response/cell defense	11
RNA processing and binding, modification	11
Immunity	8
Histocompatibility and cell surface markers	7
Cell cycle related	7
Vesicular protein trafficking and fusion, vesicular formation	7
Intracellular transporter	7
Homeostasis	7
Antivirus	5
Oncogenesis	5
Apoptosis, antiapoptosis	5
Zinc finger protein	3
Growth factor	3
Translation	3
Hormone related	1
DNA modification and replication	1
Unknown function	60
Hypothetical protein	152
Total	641

of a series of antiviral genes observed at 6 h post infection persisted until 24 h post infection. Many genes that are implicated in broad biological functions were upregulated, in particular, cellular signal transducers, such as transcription factors, zinc finger proteins, protein kinases, and phosphatases, were induced. This result suggests that, during the late stages of MV infection, MV replication strongly induces the expression of many genes that control multiple cellular functions. About half of the upregulated genes were classified as hypothetical or unidentified genes.

The number of downregulated gene in 293SLAM cells was also greatly increased 24 h post infection (Fig. 2B). A total of 641 genes were identified. Many of the downregulated genes could be classified in restricted categories (Table 2). The majority of genes that were downregulated were so-called 'housekeeping genes'. In particular, a large quantity of mitochondrial protein genes, including those involved in the electron transport system and energy metabolism, were downregulated. Furthermore, most ribosomal proteins, including mitochondrial ribosomal proteins, were downregulated. In addition, many genes implicated in the cytoskeleton, cell structure and enzymes of the glycolytic pathway and lipid metabolism were also downregulated. These observations suggest that, during later stages of infection, MV infection induced deficient maintenance of overall cellular function.

MV infection induced a biphasic modulation of gene expression in 293SLAM cells; in the early stage, a series of antiviral gene expressions were rapidly induced, and during the later stages of infection, MV replication modulated the expression of genes across a broad range of functional categories.

Effects of MV on gene expression in COBL-a cells

In COBL-a cells, only limited sets of gene expression profiles were modulated after MV infection. In fact, 24 h post infection, only 23 genes were upregulated (Table 3). In contrast to that seen in 293SLAM cells, the series of genes involved in innate antiviral responses was not altered, other than a single cytokine. This result in COBL-a cells suggests that MV suppresses expression of genes involved in the host antivirus system and the IFN-α/β signaling pathway. Only 17 genes were downregulated in COBL-a cells 24 h post infection (Table 4). Many of these genes were related to metabolic enzymes involved in sterol and fatty acid. All of these genes were also downregulated in 293SLAM cells. This suggests that the downregulation signal of MV infection was partially and weakly conserved between 293SLAM and COBL-a cells.

Effect of recombinant MV lacking V protein on gene expression

As with other paramyxoviruses, MV produces two nonstructural accessory molecules, the C and V proteins, encoded within the phosphoprotein gene. In MV, several reports have

Table 3
Upregulated at 24 h post MV infection in COBL-a cells

Gene name	cDNA accession no.	Fold increase (log2)
Dehydrogenase/reductase (SDR family) member 2 (DHRS2), mRNA	NM_005794	2.2301
Rhabdoid tumor deletion region gene 1 (RTDR1), mRNA	NM_014433	1.8515
PRO1768 protein (PRO1768), mRNA	NM_014099	1.6207
Ras protein-specific guanine nucleotide-releasing factor 1 (RASGRF1)	NM_002891	1.5769
KIAA0590 gene product (KIAA0590), mRNA	NM_014714	1.4823
cDNA FLJ30514 fis, clone BRAWH2000682	AK055076	1.4243
Titin (TTN), transcript variant novex-3	NM_133379	1.404
Crystallin, beta A1 (CRYBA1), mRNA	NM_005208	1.3464
cDNA FLJ37863 fis, clone BRSSN2015907	AK095182	1.2957
cDNA FLJ30520 fis, clone BRAWH2000866	AK055082	1.2934
LOC135666 (LOC135666), mRNA	XM_069484	1.2514
cDNA FLJ fis, clone PLACE6000414	AK122657	1.1769
cDNA FLJ31592 fis, clone NT2RI2002447	AK056154	1.141
cDNA FLJ35408 fis, clone SKNSH2008969	AK092727	1.139
Hypothetical gene supported by AF007152	XM_032158	1.1382
cDNA FLJ13701 fis, clone PLACE2000223	AK023763	1.1294
cDNA FLJ10500 fis, clone NT2RP2000369	AK001362	1.1278
Similar to IGE-BINDING PROTEIN (LOC120889), mRNA	XM_062339	1.1235
cDNA FLJ35884 fis, clone TESTI2008960	AK093203	1.0978
Similar to cellular retinaldehyde-bindin	XM_069035	1.081
cDNA FLJ fis, clone BRACE2032329	AK124476	1.0558
Transient receptor potential cation channel, subfamily V, member 4 (TRPV4)	NM_021625	1.0507
Small inducible cytokine A4 (SCY A4), mRNA	NM_002984	1.0031

shown that the V protein possesses IFN-antagonist activity. To evaluate the involvement of V protein in host gene expression during MV infection, we established a reverse genetics system for MV-HL (Yoneda et al., unpublished data). Using the infectious clone, we succeeded in generating recombinant MV lacking V protein expression. We performed a microarray analysis using the V knockout MV. As shown in Fig. 3A, V knockout MV-infected cells had a similar expression profile to that of parental MV. In 293SLAM cells, rapid induction of innate immune and antiviral responses was observed, similar to that seen during parental MV infection. At 24 h post infection, V knockout MV displayed slightly weak modulation of host gene expression, but the categories of regulated genes highly overlapped with that of parental MV. Interestingly, in COBL-a cells, no alteration of cellular gene expression, including IFN signaling, was observed with V knockout MV.

To confirm the early steps of IFN signaling during MV-HL and V knockout MV infection, we examined tyrosine phosphorylation of signal transducer and activator 1 (STAT1) which is induced by IFN response. COBL-a cells and 293SLAM cells were infected with MV-HL or V knockout MV, and the cell lysates were subjected to western blotting. As shown in Fig. 3B, similar levels of tyrosine-phosphorylated STAT1 (pY-STAT1) were detected in 293SLAM cells infected with both MV-HL and V knockout MV. On the other hand, pY-STAT1 was not detectably induced in COBL-a cells after MV-HL and V knockout MV infection. Protein levels of STAT1 did not show significant differences between uninfected and infected cells of COBL-a and 293SLAM.

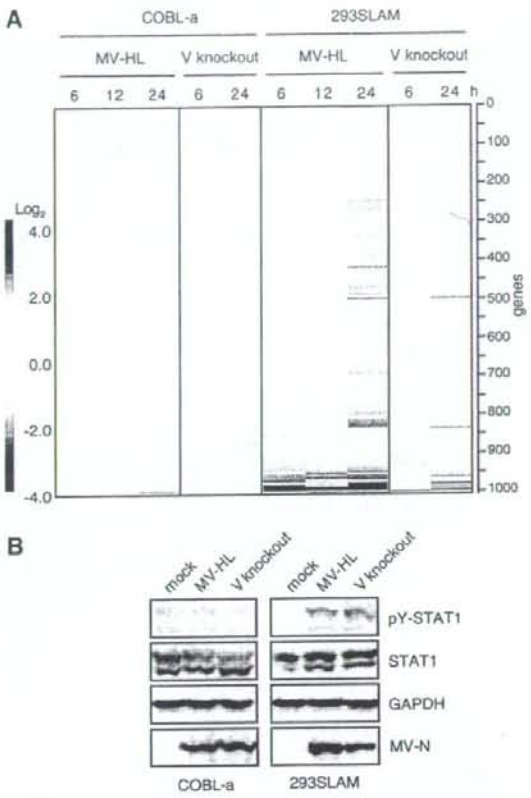

Fig. 3. Effect of recombinant MV lacking V protein on gene expression. (A) Comparison of the expression profiles between parental MV and V knockout MV. 293SLAM and COBL-a cells were inoculated with MV-HL or V knockout MV. Genes exhibiting the mean log ratio in all 10 samples were extracted (11,829 genes). These genes were further extracted with |mean log ratio| ≥ 1, and the resulting 1,012 genes were assembled in the order obtained from the results of hierarchical clustering analysis. The y-axis of the dendrogram depicts Euclid square distance as the dissimilarity coefficient. The color bar on the left side of the figure shows the expression ratio against mock-infected RNA in $\log_2$; red and blue indicate increase and decrease of mean log ratios, respectively. (B) STAT1 activating tyrosine phosphorylation was tested by western blotting with STAT1 phosphopeptide-specific antibody in COBL-a cells and 293SLAM cells infected with mock, MV-HL or V knockout MV. Total STAT1 level, GAPDH and MV-N protein expression were analyzed in parallel.

Table 4
Downregulated genes at 24 h post MV infection in COBL-a cells

Gene name	cDNA accession no.	Fold increase (log2)
Stearoyl-CoA desaturase (delta-9-desaturase) (SCD)	NM_005063	−1.4765
Sterol-C4-methyl oxidase-like (SC4MOL)	NM_006745	−1.3768
Fatty acid desaturase 2 (FADS2)	NM_004265	−1.3506
Epidermal growth factor receptor pathway substrate 8 (EPS8)	NM_004447	−1.2887
Midline 1 (Opitz/BBB syndrome) (MID1), transcript variant 1	NM_000381	−1.1804
Isopentenyl-diphosphate delta isomerase (IDI1)	NM_004508	−1.1777
7-dehydrocholesterol reductase (DHCR7)	NM_001360	−1.165
Hypothetical protein FLJ11700 (FLJ11700)	NM_024892	−1.1487
Insulin induced gene 1 (INSIG1)	NM_005542	−1.1149
Acetyl-coenzyme A acetyltransferase 2 (acetoacetyl coenzyme A thiolase)	NM_005891	−1.113
Lipase A, lysosomal acid, cholesterol esterase (Wolman disease) (LIPA)	NM_000235	−1.083
24-dehydrocholesterol reductase (DHCR24)	NM_014762	−1.0687
Cytochrome P450, 51 (lanosterol 14-alpha-demethylase) (CYP51)	NM_000786	−1.0677
LIM and cysteine-rich domains 1 (LMCD1)	NM_014583	−1.047
Sialyltransferase 1 (beta-galactoside alpha-2, 6-sialytransferase) (SIAT1)	NM_003032	−1.0333
cDNA FLJ36451 fis, clone THYMU2013757	AK093770	−1.0286
3-hydroxy-3-methylglutaryl-coenzyme A synthase 1 (soluble)	NM_002130	−1.0104

Given these data, there is little difference in host gene expression between MV-HL and V knockout MV, and V protein is considered to have little effect on changing cellular gene expression, in particular the series of genes responsible for IFN, during virus replication.

MV suppresses the IFN signaling pathway in COBL-a cells but not in 293SLAM cells

As assessed by microarray analysis, the modulation of host gene expression profile induced by MV infection was different in epithelial versus lymphoid cells. In particular, in the early period of infection, it appeared that the antiviral responses, including the expression of genes responsible for IFN, were not

induced in COBL-a cells. To confirm whether the IFN signaling pathway functions normally in COBL-a cells, we analyzed changes in gene expression that occurred in response to IFN treatment. 293SLAM cells and COBL-a cells were treated with IFN-α for 24 h, and microarray analysis was performed. The number of upregulated genes with a mean log ratio greater than 1 included 65 genes in COBL-a cells and 49 genes in 293SLAM cells; the gene expression profiles, including the upregulation of IFN-stimulated genes, was similar in these two cell lines. This result indicates that the essential IFN signaling pathway in COBL-a cells was functioning normally. Taken together with profiles after MV infection, it appears that MV infection suppressed this pathway in COBL-a cells but not 293SLAM cells. Therefore, we examined the effects of V protein expression and MV infection on IFN signaling in these two cell-types using a luciferase reporter gene which was under the control of the interferon signaling response element (ISRE). Treatment with IFN-α increased luciferase activity by about 5.6- and 4.0-fold in mock-infected 293SLAM and COBL-a cells, respectively, compared to untreated controls (Fig. 4). In both 293SLAM and COBL-a cells plasmid-expressed V protein completely abolished IFN-α induced activation of the ISRE (Fig. 4). On the other hand, in MV-infected 293SLAM cells, IFN-α-induced reporter activity was further increased and reached a 10.9-fold increase compared to untreated controls (Fig. 4), suggesting that MV-induced synergistic ISRE activation. In contrast, MV infection induced very little IFN signaling in COBL-a cells (Fig. 4), which was consistent with microarray analysis results. Interestingly, additional treatment with IFN-α did not induce synergistic activation but rather suppressed the activity of the IFN signaling pathway; there was only a 1.6-fold increase in activity in COBL-a cells compared to untreated controls (Fig. 4). These results indicate that MV infection in COBL-a cells strongly suppresses the activity of the IFN signaling pathway.

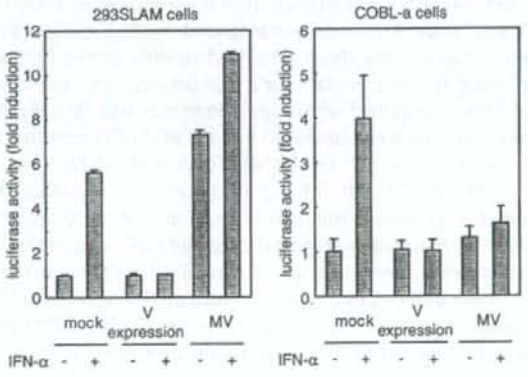

Fig. 4. MV infection inhibits IFN-α/β signaling in COBL-a but not 293SLAM cells. (A) 293SLAM cells and (B) COBL-a cells were cotransfected with an ISRE-luciferase (firefly) reporter gene, a control renilla luciferase gene, with or without V-expression plasmid. After 42 h, cells were infected with mock or MV-HL at an MOI of 2 for 6 h, and then treated with 1000 U of IFN-α per ml for 24 h. Relative expression levels were normalized by renilla luciferase activity, and the activation increase is reported as fold activation.

Discussion

We analyzed the expression of approximately 22,000 human genes during MV infection in an epithelial (293SLAM cells) and lymphoid (COBL-a cells) cell line using DNA microarrays, and identified different profiles.

In 293SLAM cells, MV infection induced rapid and strong host innate immune and antiviral responses. Host innate immune responses are the first line of defense against infections. Previously, various groups have reported that MV infection induces innate immune responses, such as: activation of NF-κB and IRF-3 transcription factors (Helin et al., 2001; Servant et al., 2001); IFN biosynthesis (Helin et al., 2001; Naniche et al., 2000); production of several cytokines (interleukin[IL]-6,-8, RANTES) (Helin et al., 2001; Sato et al., 2005); activation of IFN-stimulated gene factor 3 and GAF signaling complexes (Helin et al., 2001); induction of IRF-1 and -7 (tenOever et al., 2002; Yokota et al., 2004); and induction of immediate-early genes and genes linked to antiviral responses (Bolt et al., 2002; Helin et al., 2002). In addition to *in vitro* experiments, we have also studied the pathogenicity of MV-HL in cynomolgus monkeys, and found that type I IFN and several cytokines were transiently detected in the serum after inoculation (Sato et al., 2008). In the present study, microarray analysis clearly showed that MV infection induced innate immune and antiviral responses in 293SLAM cells, indicating that our microarray analysis was generally in agreement with previous reports. Recently, Zillox et al. reported that MV-infected dendritic cells also induced activation of antiviral responses and downregulation of housekeeping genes (Zilliox et al., 2006), coincident with our present study. A notable difference was that no induction of PKR was observed in dendritic cells (Zilliox et al., 2006) whereas, in our study, 293SLAM cells displayed clear upregulation of PKR after MV infection. This difference may be due to the cell-type.

In addition to antiviral responses, the later stage of infection showed comprehensive upregulation and downregulation of host gene expression in 293SLAM cells (Fig. 2). Previous microarray analysis reports stated that during various virus infection and replication, the genes induced by antiviral responses, such as those that are involved in the activation of NF-κB (O'Donnell et al., 2006; Tian et al., 2002) and IRF-3 (Fredericksen et al., 2004; Grandvaux et al., 2002a), were only part of the overall virus-induced gene expression profile that occurred. In addition, our data indicate that type I IFN-induced upregulation of only 49 genes in 293SLAM cells. Thus, it is likely that most of the modulated gene expression that occurs during the later stage of MV infection in 293SLAM cells is due to cellular responses to MV as a result of the accumulation of viral replication products and/or an increase in CPEs. Indeed, we used UV-inactivated MV and showed that there was no alteration of gene expression in 293SLAM cells 6 h and 24 h post inoculation (data not shown). Therefore, alteration in gene expression could not be triggered simply through signaling at the cell surface, but requires virus replication and/or accumulation of viral components in the cell. The activating signals that control expression of MV-inducible genes require further investigation.

While MV grew comparably in COBL-a and 293SLAM cells (Fig. 1), gene expression, including the expression of IFN-inducible genes, was affected very little by MV infection in COBL-a cells (Fig. 2). This result is in agreement with a previous study showing that wild-type MV had the capacity to suppress the induction of IFN-α/β in PBMCs (Naniche et al., 2000). In contrast to our microarray analysis of COBL-a cell, Bolt et al. reported that wt-MV-infected PBMCs upregulated IFN-β and IRF-7 (Bolt et al., 2002). The MV solution Bolt used contained EBV because the MV was propagated in an EBV-transformed cells. EBV probably affected the gene expression, because cytomegalovirus in the same family as EBV upregulates many cytokine gene expressions (Zhu et al., 1998). Indeed, we performed a preliminary microarray experiment using B95a-passaged MV-HL and found that several factors, including IFN-β and IRF-7, were upregulated (data not shown).

After MV infection, COBL-a cells induced low but apparent IFN levels (data not shown); however, the series of genes involved in innate antiviral responses was not upregulated (Table 3). Usually, low levels of IFN production can induce amplification of IFN production by a cellular autocrine mechanism via IFN signal transduction (Grandvaux et al., 2002b). However, in MV-infected COBL-a cells, amplification of IFN secretion was not observed. In addition, the IFN reporter assay showed that IFN-α treatment induced IFN signal transduction effectively although MV infection strongly suppressed transduction in COBL-a cells (Fig. 4). These results indicate that, in COBL-a cells, the essential IFN production capability and the IFN signaling pathway function normally, but MV infection abrogates IFN signal transduction.

It has previously been reported that the V protein of MV is involved in the inhibition of IFN signaling processes by inhibition of IFN-induced STAT nuclear translocation (Palosaari et al., 2003), the inhibition of STAT1 and STAT2 phosphorylation (Takeuchi et al., 2003), and the suppression of Jak phosphorylation (Yokota et al., 2003). We also confirmed that the V protein of MV-HL, expressed by a mammalian expression plasmid, completely suppresses IFN signaling in both 293SLAM and COBL-a cells (Fig. 4). However, as shown in Fig. 3A, in COBL-a cells, V knockout MV caused little change in cellular gene expression, including IFN signaling. The V knockout MV grew as well as the parental MV-HL (data not shown). Given these data, during virus replication, V protein appeared to have little effect on alteration of cellular gene expression, in particular the series of IFN responsible genes. Thus, in COBL-a cells, other factor(s) might also act as IFN-antagonist. In contrast, in MV-infected 293SLAM cells, IFN signaling was not blocked by MV infection (Fig. 4). Thus, V protein does not act as an IFN-antagonist or inadequately suppresses the IFN signaling pathway in MV-infected 293SLAM cells. These results indicate that plasmid-expressed V protein can interfere with IFN signal transduction in various cells including 293SLAM cells, but that during MV infection, other factors may counteract and/or overcome the inhibitory effect of V protein, depending on the specific cell-type. The mechanism of cell-type specific inhibition will need to be identified in order to clarify the function of the viral proteins during MV replication.

In addition to host antivirus responses, a number of changes in gene expression observed in 293SLAM cells 24 h post infection were not detected in COBL-a cells. Interestingly, *in vitro* MV-induced immunosuppression is cell-type dependent. The proliferation rates of lymphoid cells, such as peripheral blood leucocytes, human T-cells, B cells, and monocytic cell lines, were significantly reduced by MV infection. On the other hand, no such effects were observed in cells of nonlymphoid origin (Schlender et al., 1996). In addition, a recent study found that IFN-γ-mediated antivirus activity against MV is caused in epithelial, endothelial, and astroglial cells, but not in lymphoid and neuronal cell lines (Obojes et al., 2005). These data imply that cellular factors specific for lymphoid cells are implicated in specific responses observed during MV infection and replication. In the present paper, we focused on the analysis of IFN signal transduction suppression. In future, modification of other pathways should be analyzed in detail.

This microarray analysis will help uncover new clues for analyzing the behaviour of host genes in response to infection, and the role of viral proteins in the context of MV infection.

Materials and methods

Cell culture

B95a cells and COBL-a cells were grown in RPMI1640 medium with 100 U penicillin per ml, 100 μg streptomycin per ml, and 5% (B95a cells) or 10% (COBL-a cells) fetal calf serum (FCS), at 37 °C in a 5% CO_2 incubator. Human embryonic kidney 293 cells and their derivatives were grown in Dulbecco minimal essential medium with 10% FCS, penicillin, and streptomycin at 37 °C in a 5% CO_2 incubator.

Establishment of 293SLAM cells

In order to establish epithelial cell lines stably expressing SLAM, total RNA was isolated from B95a cells using ISOGEN (NipponGene) and reverse transcribed with SuperScript II reverse transcriptase (Invitrogen) and random primer (9-mer), according to the manufacturer's instructions. The cDNA of SLAM was amplified with a specific primer pair flanking the *Eco*RI site, and then introduced into the pCAGGS mammalian expression vector (pCAG-SLAM) (Tokui et al., 1997). One μg of pCAG-SLAM and 0.1 μg of pcDNA3.1 encoding the neomycin resistance gene (Invitrogen) were cotransfected with FuGENE6 transfection reagent (Roche) into 293 cells seeded on a 10-cm dish, according to the manufacturer's instructions. Cells were then cultured in the presence of 100 μg/ml of G418. A clone expressing the highest level of SLAM (293SLAM cells) was selected for use in the following experiments.

Virus growth

293SLAM cells and COBL-a cells (1×10^6 per six-well plate) were infected with MV-HL at an MOI of 0.001 for 1 h. The inoculum was removed, and the cells were washed once with medium and then incubated in medium containing 5% FCS.

Cells and supernatants of wells infected with MV-HL were harvested 12, 24 and 48 h later, and carried out the freezing–thawing cycle three times. Infectivity was determined by $TCID_{50}$ titration using the standard method. The experiment was repeated two times.

Generation of V knockout MV

To create V protein knockout MV, a previously established plasmid encoding the cDNA of the full-length genome of wild-type HL strain of MV was used (Yoneda et al., unpublished data). Two nucleotide substitutions (antigenome ^{2491}AAAAAGGG^{2498} to ^{2491}AAGAAGG^{2498}) were introduced into the editing site in the P gene of the plasmid to ensure that no editing would occur; the result was designated pMV-ΔV. The recombinant V knockout MV-HL was generated from pMV-ΔV. Briefly, 293 cells were placed in a 6-well culture dish, inoculated with a recombinant vaccinia virus (MVA-T7) for 1 h, and then transfected with 1 μg of pMV-ΔV, 1 μg of pKSN1, 1 μg of pKSP, and 0.3 μg of pGEML per well, which expressed N, P, and L proteins, respectively, under the control of a T7 promoter, using FuGENE6. After incubation for 3 days, the cells were co-cultivated with B95a cells at a concentration of 2×10^6 cells per well, and further incubated until extensive cytopathic effects were noted. To confirm the absence of V-expression, total RNA was reverse transcribed with oligo-dT primer, and cDNA of the P gene fragment containing the editing site (antigenome position 2401–3342) was amplified by PCR. No G residue insertion in the editing site was identified by direct sequencing (data not shown).

Preparation and purification of MVs

To eliminate EBV in the stock solution of MV-HL and recombinant V knockout MV, which had been passaged on B95a cells, primary virus solution was passaged twice in 293SLAM cells. The MV solution was inoculated into COBL-a cells cultured in a Cell Factory (Nunc) and propagated. After 3 days, the cells and culture medium were harvested, subjected to three cycles of freeze–thawing, and then centrifuged at 1,500 ×*g* for 10 min. The prepared virus solution was centrifuged in a type19 fixed angle rotor (Beckman Inc.) at 19,000 rpm for 120 min at 4 °C. Pelleted virions were resuspended in 5 ml of RPMI1640.

Preparation of RNA samples for microarray analysis

COBL-a cells and 293SLAM cells (3×10^7) were infected with MV-HL or V knockout MV at an MOI of 2. After 1 h of adsorption at 37 °C, the inocula were replaced with warm spent medium. Alternatively, both cells were treated with 1,000 IU/ml of human universal type I IFN (PBL Biomedical Laboratories). At the predetermined time after addition of the virus or IFN, the medium was removed and the cells were lysed with an ISOGEN reagent. Total RNA was prepared from the lysate in accordance with the manufacturer's instructions. Poly(A)+RNA was prepared from total RNA with a MicroPoly (A)Purist Kit (Ambion), in accordance with the manufacturer's instructions.

Microarray preparation and expression profile acquisition

DNA microarray analysis was performed as previously described (Ito et al., 2003; Kobayashi et al., 2004; Miura et al., 2006; Sakamoto et al., 2005; Yanagisawa et al., 2006). A set of synthetic polynucleotides (80-mers) that represented 22,272 human transcripts mostly originating from the RefSeq clones deposited in the NCBI database was purchased (MicroDiagnostic, Japan) and arrayed on a slide glass (coated slide glass for the microarray, type I; Matsunami, Kishiwada, Japan) with a custom-made arrayer (designated the 22K array) (Ito et al., 2003; Kobayashi et al., 2004). Poly(A)+RNA (2 μg) was labeled with SuperScript II and Cyanine 5-dUTP or Cyanine 3-dUTP (PerkinElmer). A pair of the Cyanine 5- and Cyanine 3-labeled samples was hybridized onto a single microarray. All pairs of target and control samples were labeled and hybridized to microarrays along with color flip of Cyanine 5 and Cyanine 3. Labeling, hybridization, and subsequent washes of microarrays were performed with a Labeling & Hybridization Kit (MicroDiagnostic), in accordance with the manufacturer's instructions. Hybridization signals were measured with a GenePix 4000A scanner (Axon Instruments, CA, USA) and then processed into primary expression ratios ([Cyanine 5-intensity obtained from each target or control sample]/[Cyanine 3-intensity obtained from each control or target sample], which are indicated as 'median of ratios' in GenePix Pro 3.0 software (Axon Instruments)). Normalization was performed for the median of ratios (primary expression ratios) by multiplying normalization factors calculated for each feature on a microarray by the GenePix Pro 3.0 software (designated normalized ratios). After conversion of the normalized ratios into $\log_2$ values (designated log ratios), log ratios derived from pairs of Cyanine 3-labeled target and Cyanine 5-labeled control samples were converted into reciprocals. Eventually, log ratios derived from pairs of Cyanine 5-labeled target and Cyanine 3-labeled control samples and the reciprocal log ratios derived from pairs of Cyanine 3-labeled target and Cyanine 5-labeled control samples were subjected to calculation of mean averages for individual genes (designated mean log ratios). Data processing and subsequent hierarchical clustering analysis were performed with an MDI gene expression analysis software package (MicroDiagnostic). Genes exhibiting the mean log ratio in all data sets were extracted. These genes were further extracted with mean log ratio greater than 1 or lower than −1, and the resulting genes were assembled in the order obtained from the results of hierarchical clustering analysis. All the data in accordance with the MIAME guideline were deposited at DDBJ via CIBEX (http://www.cibex.nig.ac.jp/cibex/HTML/index.html) under accession numbers CBX32.

Western blotting

293SLAM cells and COBL-a cells in 3.5 cm-diameter dish were infected with MV-HL or V knockout MV at an MOI of 2.

After 6 h of infection, cells were washed with PBS, lysed with the SDS sample buffer, and then subjected to a 30-s sonication with a Sonifier 450 (BRANSON). Cell lysate was boiled for 5 min, and then resolved on 10% SDS-PAGE gels and transferred to polyvinylidene difluoride membranes (Millipore). The membranes were incubated with a 1:1000 dilution of anti-STAT1 rabbit polyclonal antibody (Santa Cruz Biotechnology), a 1:200 dilution of anti-pY-STAT rabbit polyclonal antibody (Santa Cruz Biotechnology), a 1:1000 dilution of anti-N rabbit polyclonal antibody, or a 1:1000 dilution of anti-GAPDH mouse monoclonal antibody (CHEMICON) at 4 °C overnight. The membranes were washed three times with PBS, then incubated with a 1:2000 dilution of horseradish peroxidase-conjugated rabbit anti-mouse, or goat anti-rabbit, IgG (Dako) at room temperature for 1 h. Proteins that bound antibodies were detected by ECL Plus western blotting detection reagents (Amersham).

Luciferase reporter assays

To construct expression plasmids encoding the MV-V gene, the P gene of MV-HL was amplified with specific primer pairs containing the *Eco*RI sequence flanking its 5' terminus and inserted into the *Eco*RI site of the pCAGGS eukaryotic expression vector, and then introduced specific insertion of G residues at the editing site by a PCR-based mutagenesis technique using the QuikChange site-directed mutagenesis kit (Stratagene) (pCAG-V). 293SLAM cells were seeded at 2×10^5 cells per well of a 24-well tissue culture plate and then transiently cotransfected with 0.1 μg of pISRE-Luc, 10 ng of pRL-CMV (Promega) with or without 1.2 μg of pCAG-V using FuGENE6. COBL-a cells were seeded at 4×10^5 cells per well of a 24-well plate and transiently cotransfected with 1 μg of pISRE-Luc, 20 ng of pRL-CMV, and with or without 2.4 μg of pCAG-V using Lipofectamine2000 (Invitrogen) according to the manufacturer's protocol. After 42 h, cells were infected with mock or MV at an MOI of 2 for 6 h, and then treated with 1,000 IU/ml of human universal type I IFN and incubated for 24 h. Cells were lysed with passive lysis buffer (Promega), and luciferase activity was measured using Dual-luciferase reporter assay system (Promega). Experiments were performed in triplicate.

Acknowledgments

This study was supported by a grant from the Program for Promotion of Basic Research Activities for Innovative Biosciences (PROBRAIN), and a grants-in-aid from the Ministry of Education, Science, Culture, and Sports, Japan.

References

Bolt, G., Berg, K., Blixenkrone-Moller, M., 2002. Measles virus-induced modulation of host-cell gene expression. J. Gen. Virol. 83 (Pt 5), 1157–1165.

Dhib-Jalbut, S.S., Cowan, E.P., 1993. Direct evidence that interferon-beta mediates enhanced HLA-class I expression in measles virus-infected cells. J. Immunol. 151 (11), 6248–6258.

Fredericksen, B.L., Smith, M., Katze, M.G., Shi, P.Y., Gale Jr., M., 2004. The host response to West Nile virus infection limits viral spread through the activation of the interferon regulatory factor 3 pathway. J. Virol. 78 (14), 7737–7747.

Grandvaux, N., Servant, M.J., tenOever, B., Sen, G.C., Balachandran, S., Barber, G.N., Lin, R., Hiscott, J., 2002a. Transcriptional profiling of interferon regulatory factor 3 target genes: direct involvement in the regulation of interferon-stimulated genes. J. Virol. 76 (11), 5532–5539.

Grandvaux, N., tenOever, B.R., Servant, M.J., Hiscott, J., 2002b. The interferon antiviral response: from viral invasion to evasion. Curr. Opin. Infect. Dis. 15 (3), 259–267.

Griffin, D.E., 2001. Measles virus. Fields Virology, 3rd ed. Lippincott Williams& Wilkins, pp. 1401–1441.

Helin, E., Matikainen, S., Julkunen, I., Heino, J., Hyypia, T., Vainionpaa, R., 2002. Measles virus enhances the expression of cellular immediate-early genes and DNA-binding of transcription factor AP-1 in lung epithelial A549 cells. Arch. Virol. 147 (9), 1721–1732.

Helin, E., Vainionpaa, R., Hyypia, T., Julkunen, I., Matikainen, S., 2001. Measles virus activates NF-kappa B and STAT transcription factors and production of IFN-alpha/beta and IL-6 in the human lung epithelial cell line A549. Virology 290 (1), 1–10.

Ito, E., Honma, R., Imai, J., Azuma, S., Kanno, T., Mori, S., Yoshie, O., Nishio, J., Iwasaki, H., Yoshida, K., Gohda, J., Inoue, J., Watanabe, S., Semba, K., 2003. A tetraspanin-family protein, T-cell acute lymphoblastic leukemia-associated antigen 1, is induced by the Ewing's sarcoma–Wilms' tumor 1 fusion protein of desmoplastic small round-cell tumor. Am. J. Pathol. 163 (6), 2165–2172.

Kobayashi, S., Ito, E., Honma, R., Nojima, Y., Shibuya, M., Watanabe, S., Maru, Y., 2004. Dynamic regulation of gene expression by the Flt-1 kinase and matrigel in endothelial tubulogenesis. Genomics 84 (1), 185–192.

Kobune, F., Sakata, H., Sugiura, A., 1990. Marmoset lymphoblastoid cells as a sensitive host for isolation of measles virus. J. Virol. 64 (2), 700–705.

Kobune, F., Takahashi, H., Terao, K., Ohkawa, T., Ami, Y., Suzaki, Y., Nagata, N., Sakata, H., Yamanouchi, K., Kai, C., 1996. Nonhuman primate models of measles. Lab. Anim. Sci. 46 (3), 315–320.

Kobune, F., Ami, Y., Katayama, M., Takahashi, M., Tuul, R., Korukluoglu, G., Kiyohara, T., Miura, R., Sato, H., Yoneda, M., Kai, C., 2007. A novel monolayer cell line derived from human umbilical cord blood cells shows high sensitivity to measles virus. J. Gen. Virol. 88, 1565–1567.

Miura, A., Honma, R., Togashi, T., Yanagisawa, Y., Ito, E., Imai, J., Isogai, T., Goshima, N., Watanabe, S., Nomura, N., 2006. Differential responses of normal human coronary artery endothelial cells against multiple cytokines comparatively assessed by gene expression profiles. FEBS Lett. 580 (30), 6871–6879.

Naniche, D., Yeh, A., Eto, D., Manchester, M., Friedman, R.M., Oldstone, M.B., 2000. Evasion of host defenses by measles virus: wild-type measles virus infection interferes with induction of Alpha/Beta interferon production. J. Virol. 74 (16), 7478–7484.

Noe, K.H., Cenciarelli, C., Moyer, S.A., Rota, P.A., Shin, M.L., 1999. Requirements for measles virus induction of RANTES chemokine in human astrocytoma-derived U373 cells. J. Virol. 73 (4), 3117–3124.

O'Donnell, S.M., Holm, G.H., Pierce, J.M., Tian, B., Watson, M.J., Chari, R.S., Ballard, D.W., Brasier, A.R., Dermody, T.S., 2006. Identification of an NF-kappaB-dependent gene network in cells infected by mammalian reovirus. J. Virol. 80 (3), 1077–1086.

Obojes, K., Andres, O., Kim, K.S., Daubener, W., Schneider-Schaulies, J., 2005. Indoleamine 2,3-dioxygenase mediates cell type-specific anti-measles virus activity of gamma interferon. J. Virol. 79 (12), 7768–7776.

Ohno, S., Ono, N., Takeda, M., Takeuchi, K., Yanagi, Y., 2004. Dissection of measles virus V protein in relation to its ability to block alpha/beta interferon signal transduction. J. Gen. Virol. 85 (Pt 10), 2991–2999.

Palosaari, H., Parisien, J.P., Rodriguez, J.J., Ulane, C.M., Horvath, C.M., 2003. STAT protein interference and suppression of cytokine signal transduction by measles virus V protein. J. Virol. 77 (13), 7635–7644.

Sakamoto, A., Imai, J., Nishikawa, A., Honma, R., Ito, E., Yanagisawa, Y., Kawamura, M., Ogawa, R., Watanabe, S., 2005. Influence of inhalation anesthesia assessed by comprehensive gene expression profiling. Gene 356, 39–48.

Sato, H., Kobune, F., Ami, Y., Yoneda, M., Kai, C., 2008. Immune responses against measles virus in cynomolgus monkeys. Comp. Immunol. Microbiol. Infect. Dis. 31, 25–35.

Sato, H., Miura, R., Kai, C., 2005. Measles virus infection induces interleukin-8 release in human pulmonary epithelial cells. Comp. Immunol. Microbiol. Infect. Dis. 28 (4), 311–320.

Schlender, J., Schnorr, J.J., Spielhoffer, P., Cathomen, T., Cattaneo, R., Billeter, M.A., ter Meulen, V., Schneider-Schaulies, S., 1996. Interaction of measles virus glycoproteins with the surface of uninfected peripheral blood lymphocytes induces immunosuppression in vitro. Proc. Natl. Acad. Sci. U. S. A. 93 (23), 13194–13199. (see comment).

Schneider-Schaulies, J., Schneider-Schaulies, S., Ter Meulen, V., 1993. Differential induction of cytokines by primary and persistent measles virus infections in human glial cells. Virology 195 (1), 219–228.

Servant, M.J., ten Oever, B., LePage, C., Conti, L., Gessani, S., Julkunen, I., Lin, R., Hiscott, J., 2001. Identification of distinct signaling pathways leading to the phosphorylation of interferon regulatory factor 3. J. Biol. Chem. 276 (1), 355–363.

Takeuchi, K., Kadota, S.I., Takeda, M., Miyajima, N., Nagata, K., 2003. Measles virus V protein blocks interferon (IFN)-alpha/beta but not IFN-gamma signaling by inhibiting STAT1 and STAT2 phosphorylation. FEBS Lett. 545 (2–3), 177–182.

Tatsuo, H., Ono, N., Yanagi, Y., 2001. Morbilliviruses use signaling lymphocyte activation molecules (CD150) as cellular receptors. J. Virol. 75 (13), 5842–5850.

Teng, Z.P., Ooka, T., Huang, D.P., Zeng, Y., 1996. Detection of Epstein–Barr Virus DNA in well and poorly differentiated nasopharyngeal carcinoma cell lines. Virus Genes 13 (1), 53–60.

tenOever, B.R., Servant, M.J., Grandvaux, N., Lin, R., Hiscott, J., 2002. Recognition of the measles virus nucleocapsid as a mechanism of IRF-3 activation J. Virol. 76 (8), 3659–3669. (erratum appears in J Virol 2002 Jun;76(12):6413).

Tian, B., Zhang, Y., Luxon, B.A., Garofalo, R.P., Casola, A., Sinha, M., Brasier, A.R., 2002. Identification of NF-kappaB-dependent gene networks in respiratory syncytial virus-infected cells. J. Virol. 76 (13), 6800–6814.

Tokui, M., Takei, I., Tashiro, F., Shimada, A., Kasuga, A., Ishii, M., Ishii, T., Takatsu, K., Saruta, T., Miyazaki, J., 1997. Intramuscular injection of expression plasmid DNA is an effective means of long-term systemic delivery of interleukin-5. Biochem. Biophys. Res. Commun. 233 (2), 527–531.

Vidalain, P.O., Laine, D., Zaffran, Y., Azocar, O., Servet-Delprat, C., Wild, T.F., Rabourdin-Combe, C., Valentin, H., 2002. Interferons mediate terminal differentiation of human cortical thymic epithelial cells. J. Virol. 76 (13), 6415–6424.

Yanagisawa, Y., Sato, Y., Asahi-Ozaki, Y., Ito, E., Honma, R., Imai, J., Kanno, T., Kano, M., Akiyama, H., Sata, T., Shinkai-Ouchi, F., Yamakawa, Y., Watanabe, S., Katano, H., 2006. Effusion and solid lymphomas have distinctive gene and protein expression profiles in an animal model of primary effusion lymphoma. J. Pathol. 209 (4), 464–473.

Yokota, S., Saito, H., Kubota, T., Yokosawa, N., Amano, K., Fujii, N., 2003. Measles virus suppresses interferon-alpha signaling pathway: suppression of Jak1 phosphorylation and association of viral accessory proteins, C and V, with interferon–alpha receptor complex. Virology 306 (1), 135–146.

Yokota, S., Okabayashi, T., Yokosawa, N., Fujii, N., 2004. Growth arrest of epithelial cells during measles virus infection is caused by upregulation of interferon regulatory factor 1. J. Virol. 78 (9), 4591–4598.

Zhu, H., Cong, J.P., Mamtora, G., Gingeras, T., Shenk, T., 1998. Cellular gene expression altered by human cytomegalovirus: global monitoring with oligonucleotide arrays. Proc. Natl. Acad. Sci. U.S.A. 95 (24), 14470–14475.

Zilliox, M.J., Parmigiani, G., Griffin, D.E., 2006. Gene expression patterns in dendritic cells infected with measles virus compared with other pathogens. Proc. Natl. Acad. Sci. U. S. A. 103 (9), 3363–3368.

Antiviral Research 80 (2008) 370–376

Contents lists available at ScienceDirect

Antiviral Research

journal homepage: www.elsevier.com/locate/antiviral

Heparin-like glycosaminoglycans prevent the infection of measles virus in SLAM-negative cell lines

Yuri Terao-Muto, Misako Yoneda, Takahiro Seki, Akira Watanabe, Kyoko Tsukiyama-Kohara, Kentaro Fujita, Chieko Kai*

Laboratory Animal Research Center, Institute of Medical Science, The University of Tokyo, 4-6-1 Sirokanedai, Minato-ku, Tokyo 108-8639, Japan

ARTICLE INFO

Article history:
Received 7 February 2008
Received in revised form 7 August 2008
Accepted 26 August 2008

Keywords:
Measles virus
Heparan sulphate
Hemagglutinin
SLAM-negative cells

ABSTRACT

The wide tissue tropism of the measles virus (MV) suggests that it involves ubiquitously expressed molecules. We have constructed a recombinant MV expressing the enhanced green fluorescent protein (EGFP) (rMV-EGFP) and demonstrated that the rMV-EGFP infected several cell types (HEK-293, HepG2, Hep3B, Huh7, and WRL68 cells) that do not express the human signalling lymphocyte activation molecule (SLAM), which is known as a cellular receptor for morbilliviruses. MV infection of HEK-293 and HepG2 cells was not inhibited in an infectivity-inhibition assay using an anti-SLAM monoclonal antibody, indicating that MV could infect cells without using SLAM. Soluble heparin (HP) inhibited the rMV-EGFP infectivity in SLAM-negative cell lines in a dose-dependent manner. Direct interaction between purified virions and HP was detected in a surface plasmon resonance assay. We also demonstrated that the hemagglutinin (H) protein, but not the fusion (F) protein is responsible for the interaction between the virions and HP. Taken together, our results suggest that HP-like glycosaminoglycans bind to the H protein of MV and play a key role in the infection of SLAM-negative cells.

1. Introduction

Measles virus (MV) is a single-stranded, negative-sense RNA virus that is classified in the genus *Morbillivirus* of the family *Paramyxoviridae*, which includes canine distemper virus (CDV), rinderpest virus (RPV), and peste des petits ruminants virus. MV propagates in lymphoid organs throughout the body. In addition, it also spreads to a wide variety of other organs, including skin, conjunctivae, kidney, lungs, gastrointestinal tract, respiratory mucosa, genital mucosa, and liver (Griffin, 2007). The two MV envelope glycoproteins H and F work in combination to elicit the fusion of virus with the cell membrane. The signalling lymphocyte activation molecule (SLAM) (also known as CD150), which is a receptor involved in T cell activation (Cocks et al., 1995), is a cellular receptor for MV (Tatsuo et al., 2000) and can be used by both the vaccine strains and wild-type strains. Vaccine strains of MV also efficiently infect cells via CD46 (Dörig et al., 1993; Naniche et al., 1993), a ubiquitously expressed regulator of complement activation. Binding of the virus to the target cells is a critical factor for determining the tissue tropism and pathogenesis of the virus. However, it has been shown that SLAM is specifically expressed only in some T and B cells, thymocytes and dendritic cells (DCs) (Yanagi et al., 2002). Increasing evidence suggests the presence of receptors other than SLAM and CD46 for MV, and considering the wide tissue tropism of MV, ubiquitous molecules on the cell surface are expected to be involved in the attachment of MV (Hashimoto et al., 2002; Andres et al., 2003; Takeuchi et al., 2003; Takeda et al., 2007; Tahara et al., 2008).

Glycosaminoglycans are unbranched polysaccharides that are ubiquitously present on cell surfaces. Apart from their diverse functions in biologic processes by binding to various proteins including growth factors, chemokines, extracellular matrix proteins and cell adhesion molecules, they have been shown to play important roles in the cell-surface binding of pathogens such as bacteria, parasites and viruses (DeAngelis, 2002; Vogt et al., 2003; Lee et al., 2006). Recent studies demonstrated the involvement of heparin (HP)-like molecules in RPV and CDV infections (Baron, 2005; Fujita et al., 2007). However, it has been reported that infection by the Edmonston strain of MV was not inhibited by HP (Feldman et al., 2000). In the present study, we constructed a recombinant MV (HL strain) expressing the enhanced green fluorescent protein (EGFP) (rMV-EGFP), and examined whether HP-like molecules are involved in the infection of wild-type MV.

* Corresponding author. Tel.: +81 3 5449 5520; fax: +81 3 5449 5379.
E-mail address: ckai@ims.u-tokyo.ac.jp (C. Kai).

0166-3542/$ – see front matter © 2008 Elsevier B.V. All rights reserved.
doi:10.1016/j.antiviral.2008.08.006

2. Materials and methods

2.1. Cells and viruses

B95a cells (Kobune et al., 1990) were cultured in RPMI 1640 medium (SIGMA) containing 10% fetal calf serum (FCS). Human embryonic kidney (HEK)-293 cells, 293/SLAM cells expressing marmoset SLAM (Sato et al., 2008), and four liver cell lines (HepG2, Hep3B, Huh7, and WRL68) were grown in Dulbecco's modified minimum essential medium (Life Technologies Inc.) supplemented with 10% FCS. The HL strain of MV, a wild-type strain that was originally isolated from a patient, were grown in B95a cells. Recombinant viruses were obtained by using the methods described below. MV-HL and the recombinant viruses were propagated in B95a cells that were grown in 2% FCS-supplemented RPMI 1640 medium.

2.2. Rescue of rMV-EGFP

A full-length cDNA of the MV-HL genome was constructed from clones containing each of the individual genes. MV RNA was extracted from infected cells as previously described (Radecke et al., 1995). RT-PCR was performed using Superscript II reverse transcriptase (Invitrogen). All cloning procedures were conducted following standard protocols. PCR amplifications were performed using LA-Taq DNA polymerase (TAKARA) or Pfu DNA polymerase (STRATAGENE). The leader and trailer sequences were amplified using primers including EagI and EcoRI sites (leader), and EcoRI and BsmI sites (trailer). Each fragment was digested by EcoRI and EagI or BsmI, and cloned into pMDB1 using the EcoRI and EagI or BsmI sites, respectively. Amplification of the six MV genes was performed with primers containing unique restriction sites: N (NotI–FseI), P (FseI–PmeI), M (PmeI–MluI), F (MluI–SgfI), H (SgfI–AscI) and L (AscI–BsiWI). Each site was introduced immediately after the terminal codon, except that the NotI site was introduced immediately before the initiation codon of the N gene. We obtained at least 4 clones from each amplification and confirmed that the sequence in each was identical. The fragments were joined using the unique enzyme site and the sequence of the joined fragments was confirmed. Finally, the assembled genes were excised with NotI and BsiWI, and were inserted into the pMDB1 plasmid with the leader and trailer sequences. The resulting plasmid was designated pMV-HL (7+).

For construction of the full-length genome plasmid to express the enhanced green fluorescent protein, the EGFP gene was amplified from pEGFP-N1 (Clonetech) using the following primers EGFP-F; 5′-TATAGGCCGGCCATCATTGTTATAAAAAACTT AGGAACCAGGTTCATCCACAATGGTGAGCAAGGGCGAGGAGCT-3′ and EGFP-R; 5′-AAGGCCGGCCCTACTTGTACAGCTCGTCCA (FseI site in italic). The EGFP fragment was cloned into the FseI site of the pMV-HL (7+).

For recovery of rMV-EGFP from cDNA, HEK-293 cells were seeded into 6-well plates (8×10^5 cells per well) 1 day before infection and transfection. The cells were infected with replication-deficient MVAGKT7 vaccinia virus in DMEM supplemented with 2% FCS 1 h before transfection. Prior to transfection, 9 μl of Fugene 6 (Roche) were mixed and incubated with 300 μl serum-free DMEM for 5 min. Plasmids (1 μg of pMV-HL (7+), pKS-N and pKS-P, and 0.03 μg of pGEM-L (Baron and Barrett, 1997)) were mixed into 100 μl. The plasmid mixtures were then carefully pipetted into the diluted Fugene 6. MVAGKT7 was removed from the cells and replaced with 2 ml of maintenance medium containing the plasmids and Fugene 6. After 4 days' incubation, the medium was removed and 1×10^6 cells/well of B95a were added with 2 ml of RPMI1640 containing 2% FCS. When an advanced cytopathic effect was observed (usually 2–4 days after co-cultivation), the cells and medium were harvested and stored at −80 °C.

2.3. Inhibition of infection by antibodies

B95a, HEK-293, and 293/SLAM cells (1×10^4 cells) were grown in 96-well plates overnight. They were then incubated at 37 °C in medium containing 10 μg/ml of an anti-human CD46 monoclonal antibody (MAb) (clone M75: HyCult biotechnology), or an anti-human SLAM MAb (clone IPO-3: Kamiya Biomedical). At 1 h after treatment with MAbs, the cells were infected with rMV-EGFP ($TCID_{50}$ 1×10^4) at a multiplicity of infection (MOI) of 1 $TCID_{50}$/cell. At 40 h after the infection, the number of EGFP-expressing cells was counted at 20 fields under a fluorescence microscope (Olympus, IX70), and the percentage of EGFP-positive cells was calculated.

2.4. Inhibition of infection by soluble HP

For the infection–inhibition assay, rMV-EGFP ($TCID_{50}$ 1×10^5) at an MOI of 2 $TCID_{50}$/cell was inoculated at various concentrations into HEK-293 or 293/SLAM cells (2.5×10^4) in the presence of HP (Sigma). Following incubation for 40 h at 37 °C, the cells were harvested and analyzed by performing FACS using FACScan (Beckton Dickinson). In this analysis, 1×10^4 cells were counted for each sample, and the infected cells were detected by fluorescence intensity set on a log scale. Percentage of inhibition of infection was calculated relative to the extent of infection in control assays performed in the absence of HS.

2.5. Purification of the rMV-EGFP

The B95a cells infected with rMV-EGFP were subjected to 3 cycles of freezing and thawing, followed by centrifugation to remove the cell debris. The supernatant was concentrated by using a size exclusion (100-K) membrane filter (Amicon) and was loaded onto a 20–60% sucrose density gradient. Following centrifugation at 100,000 × g and 4 °C for 2 h, the virus layer was collected and applied onto a gel-filtration column (PD-10; Pharmacia) to exchange the buffer with 20 mM sodium phosphate buffer (pH 7.4).

2.6. HP affinity chromatography

For affinity chromatography, purified rMV-EGFP obtained from the infected B95a cells was used. Following equilibration of HP-agarose beads or bovine serum albumin (BSA)-agarose beads (Sigma) in phosphate-buffered saline (PBS), the concentrated virus supernatant was added to the beads, and the mixture was incubated for 30 min at 4 °C and subsequently centrifuged at 1000 × g for 1 min. The beads were washed 7 times in 1 ml PBS, followed by elution in PBS containing 2 M NaCl. The final wash and elution fractions were concentrated by using a 100-K membrane filter (VIVASPIN; Sartorius) and analyzed by SDS–PAGE followed by western blot analysis with an MAb against the N protein of MV.

To express F or H of MV, open-reading frames (ORFs) of F and H were amplified by RT-PCR and cloned into pCAGGS and pCMV-myc, respectively. The H protein expressed in pCMV-myc vector contained the N-terminal myc epitope tag. The resulting plasmids were transfected into HEK-293 cells using Fugene 6 as a transfection reagent according to the Manufacturer's instructions. At 48 h after transfection, the cells were lysed in lysis buffer (20 mM sodium phosphate (pH 7.4) containing 150 mM NaCl and 1% Triton X-100). Then, the lysates were mixed with the beads equilibrated in the lysis buffer and incubated for 1 h at 4 °C and beads were washed in the lysis buffer (7 times, with 1 ml each time), and the bound materials were eluted with increasing concentrations of NaCl in

the lysis buffer (stepwise gradient: 250 mM, 500 mM, 1 M, and 2 M). The eluted fractions were concentrated by using a 5-K membrane filter (VIVASPIN, Sartorius) and were then analyzed by SDS–PAGE followed by western blot analysis with an anti-myc or anti-MV-F MAb (see below).

2.7. Surface plasmon resonance binding assays performed using BIAcore technology

Surface plasmon resonance (SPR) measurements were performed on a BIAcore X instrument (BIAcore AB). HP (16 kDa, derived from porcine intestinal mucosa (Sigma); 100 μg/ml in 10 mM acetate buffer (pH 4.0)) was covalently immobilized to the dextran matrix of a CM5 sensor chip (Fc1) via its primary amine groups (amine coupling kit, BIAcore AB) at a flow rate of 5 μl/min (Fc1-HP). No protein was immobilized on the other side of CM5 sensor chip (Fc2) for negative control (Fc2-NC). After coating on sensor chips, we performed the masking treatment with ethanol-amine for blocking non-specific binding on sensor chip. rMV-EGFP that had been purified over a sucrose density gradient was diluted in Hanks' balanced salt (HBS) buffer (10 mM HEPES (pH 7.4), 150 mM NaCl, 3 mM EDTA, 0.005% (v/v) surfactant P20; BIAcore AB) and duplicate analyses were performed using 10 μg/ml of the virus. All affinity measurements were performed at room temperature in HBS with a constant flow rate of 20 μl/min and an injected sample volume of 40 μl. Between measurements, the chip surface was regenerated by using 100 mM HCl. Kinetic constants were determined by using the BIAevaluation 2.1 software (BIAcore X). The association, dissociation, and regeneration phases were tracked in real time by monitoring the changes in the signal expressed in resonance units (RU).

2.8. Generation of monoclonal antibodies

To produce recombinant F protein in *E.coli*, the ORF of MV-F was amplified using the following primers: MV-F F; 5′-ATGGGTCTCAAGGTGAACGT-3′ and MV-F R; 5′-TCAGAGCGACCTTACATAGG-3′, and the DNA fragment was inserted into pQE-30 (QIAGEN). Protein expression was carried out in the *E.coli* strain M15. The N-terminally His-tagged F protein was purified by Ni–NTA column (QIAGEN) according to the manufacturer's protocols with AKTA prime FPLC (Amersham Bioscience).

BALB/c mice were immunized three times with the purified F protein mixed with RIBI adjuvant (Corixa). The anti-MV-F antibody titer was assessed by performing an ELISA using the recombinant F protein as the antigen. When high anti-F antibody titers were detected in their sera, the mice were euthanized, and spleen cells were obtained. The spleen cells were fused with myeloma PAI cells, using PEG1500 (Roche). Hybridoma cells were selected by using hypoxanthine–aminopterin–thymidine (HAT) medium (Gibco BRL), and the culture supernatants were examined by immunofluorescence assay (IFA), using B95a cells infected with the HL strain of MV. Hybridomas producing anti-F antibodies were propagated and inoculated into the peritoneal cavity of BALB/c mice that had been treated with pristan (Sigma–Aldrich). At approximately 10 days after inoculation, ascites fluid was collected.

3. Results

3.1. Recovery of rMV-EGFP

The pMV plasmid containing the full-length cDNA of MV was manipulated to include unique restriction sites in the noncoding regions between adjacent genes in the MV genome. Coding regions of EGFP gene were attached to the transcription signal units (the transcription termination/polyadenylation signal of the N gene and the transcription start signal of the H gene), and cloned into the FseI site of pMV, which was inserted immediately downstream to the N gene of MV (Fig. 1A). The resulting plasmid, pMV-EGFP, was cotransfected along with supporting plasmids carrying the N, P, and L proteins of RPV into HEK-293 cells that were preinfected with the recombinant vaccinia virus MVAGKT7 expressing phage T7 RNA polymerase. The cells were incubated for 3 days, followed by cocultivation with B95a cells. Following incubation for several days, syncytia induced by the recombinant MVs were observed. The sizes of the syncytia produced by the wild-type (wt) MV (HL strain) and rMV-EGFP were similar (Fig. 1B). The growth kinetics of rMV-EGFP was comparable to that of wt MV (data not shown).

3.2. Infection of SLAM-negative cells with rMV-EGFP

We analyzed the permissibility of many cell lines to MV by using rMV-EGFP, and observed that most of these cell lines are infected with rMV-EGFP, although the levels of infection were different among cell lines (data not shown). Representatively, the HEK-293 and HepG2 cells, which do not express SLAM, exhibited specific fluorescence (Fig. 2b and d). Since wt MV does not enter cells via CD46, which is a receptor for the vaccine strain MV-Ed, our results indicate that wt MV (HL strain) can infect cells independently of SLAM and CD46. To examine whether these two known receptors, namely, SLAM and CD46, were involved in entry of the virus into these cells, we treated the cells with antibodies against these receptors followed by infection with rMV-EGFP. Pretreatment of B95a and 293/SLAM cells, which constitutively express marmoset SLAM, with a SLAM-specific MAb (IPO-3) strongly suppressed the rMV-EGFP infection (Fig. 2e and g). In contrast, pretreatment with IPO-3 did not inhibit the rMV-EGFP infection in HEK-293 and HepG2 cells (Fig. 2f and h). Furthermore, pretreatment with an MAb against CD46 (M75) did not influence the infectivity of rMV-EGFP in any of the cell lines tested (Fig. 2i–l). Therefore, it was suggested that rMV-EGFP utilize SLAM but not CD46 as a receptor, and rMV-EGFP infects SLAM-negative cells via unknown receptor(s). These results are consistent with the previous studies demonstrating the presence of alternative entry pathway(s), independent of SLAM and CD46 (Hashimoto et al., 2002; Takeuchi et al., 2003; Takeda et al., 2007; Tahara et al., 2008).

3.3. The effect of soluble HP on rMV-EGFP infection

To test whether HP-like molecules are involved in the alternative entry pathway of MV, cells were infected with rMV-EGFP in the presence of soluble HP (100 μg/ml). Not only HEK-293, 293/SLAM and HepG2 cells but also Hep3B, Huh7, and WRL68 cells were tested since MV exhibited high infectivity of MV in these cells. The number of EGFP-positive cells was counted by performing fluorescence-activated cell sorting (FACS) analysis, and the infectivity relative to that in 293/SLAM in the absence of HP was calculated. HP treatment dramatically decreased the infectivity of rMV-EGFP in HEK-293, HepG2, He3B, Huh7 and WRL68 cells by 83%, 72%, 87%, 71% and 97%, respectively (Fig. 3A). The effect of HP treatment on infection of 293/SLAM cells was small (3% reduction), probably because SLAM is a strong receptor and enables the maximum infection of MV. Thus, HP is capable of inhibiting MV infection in SLAM-negative cells.

To analyze the dose dependence, HEK-293 cells were infected with different MOIs of rMV-EGFP in the presence of increasing concentrations of HP (10, 100, and 1000 μg/ml). The infectivity at MOI 4 in the absence of HP was set as 100%. The treatment of rMV-EGFP with HP even at a low concentration of 10 μg/ml significantly inhibited the infection of the HEK-293 cells (by ~25%) and the percent inhibition increased in a dose-dependent manner (Fig. 3B). The

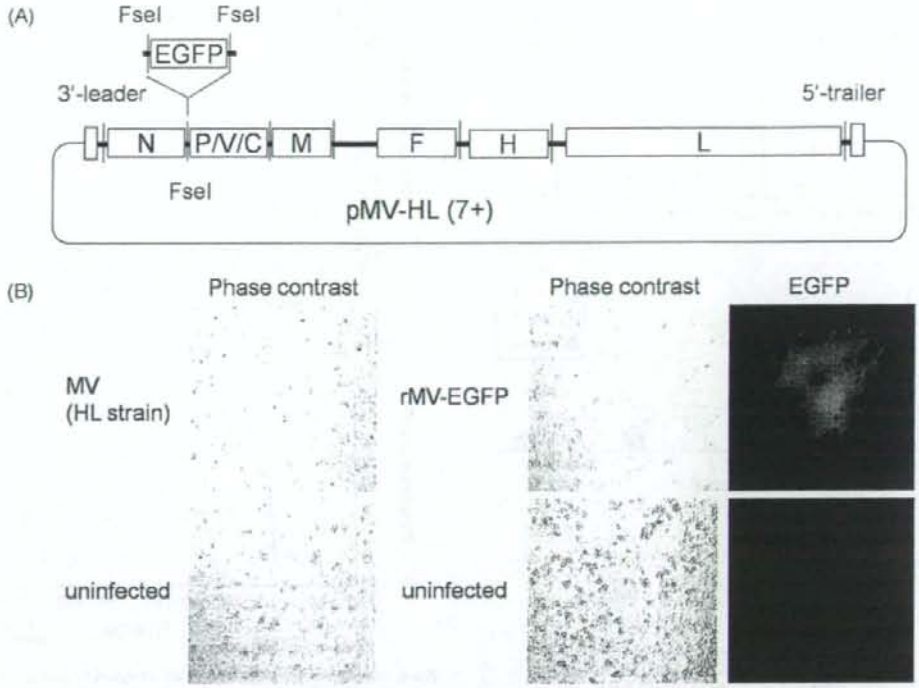

Fig. 1. (A) Construction of rMV-EGFP. The coding regions for MV structural proteins are indicated by opened boxes. The EGFP open-reading frame (ORF) fragment flanked by restriction sites for FseI was introduced into the pMV plasmid. (B) Syncytium formation in B95a cells infected with wild-type MV (HL-strain) (left) or rMV-EGFP (right). EGFP expression in the rMV-EGFP-infected B95a cells was observed under a confocal microscope (200×). Phase contrast or immunofluorescence images of uninfected cells are shown in the bottom.

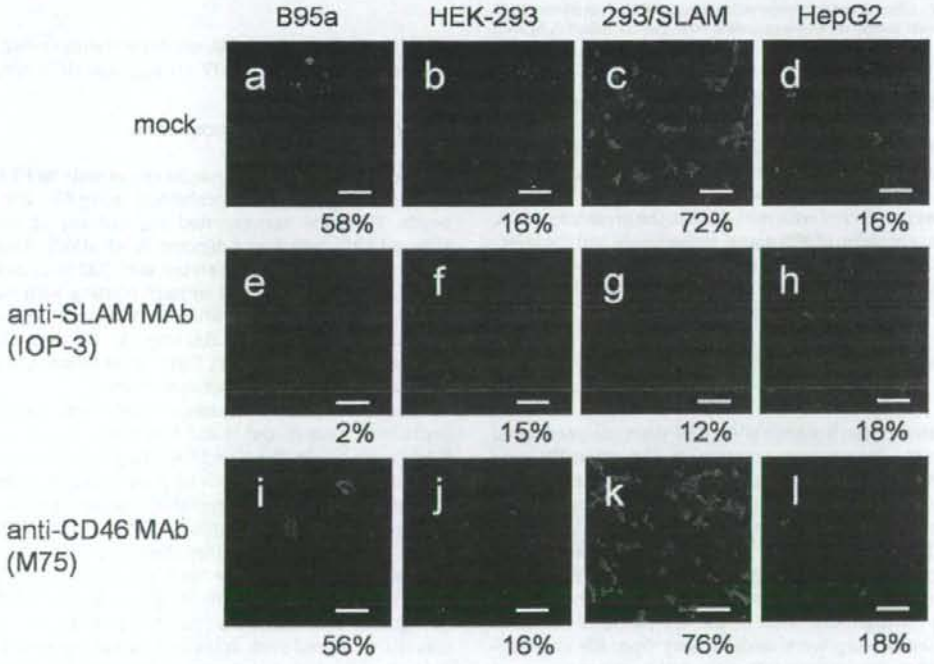

Fig. 2. (A) Effects of the anti-SLAM and anti-CD46 MAbs on rMV-EGFP infection of each cells. B95a (a, e, and i), HEK-293 (b, f, and j), 293/SLAM (c, g, and k) and HepG2 (d, h, and l) cells were pretreated with either an anti-SLAM MAb (IPO-3) (e–h) or an anti-CD46 MAb (M75) (I–l) and were subsequently infected with 10^4 $TCID_{50}$ of rMV-EGFP. At 40 h after the infection, EGFP fluorescence was observed under a fluorescence microscope (100×). The % cells infected is indicated under the panels. Bars, 100 μm.